Research Square

Preprints are preliminary reports that have not undergone peer review.
They should not be considered conclusive, used to inform clinical practice,
or referenced by the media as validated information.

Structural and mechanistic effects in one-electron oxidation of model disulfides

Monika Borkowska
Adam Mickiewicz University in Poznań
Piotr Filipiak
Adam Mickiewicz University in Poznań
Marta Teresa Ignasiak-Kciuk
Adam Mickiewicz University in Poznań
Michael J. Davies
University of Copenhagen
Tomasz Pedzinski
tomekp@amu.edu.pl

Adam Mickiewicz University in Poznań

Research Article

Keywords: Disulfide oxidation, sulfur radical-cation, photooxidation, laser flash photolysis, protein oxidation, disulfide bond cleavage

Posted Date: November 3rd, 2026

DOI: https://doi.org/10.21203/rs.3.rs-11375573/v1

License: This work is licensed under a Creative Commons Attribution 4.0 International License.
Read Full License

Additional Declarations: No competing interests reported.

Abstract

Disulfide bonds are abundant and critical structural elements that stabilize approximately 21% of all proteins, yet their oxidative degradation pathways remain significantly less characterized than their thiol precursor, cysteine, and the thioether methionine. This study employed nanosecond laser flash photolysis (LFP) and high-resolution LC-MS/MS to elucidate the mechanism of the one-electron photooxidation of two model disulfides - the cyclic species trans-4,5-dihydroxy-1,2-dithiane (DHDT) and the linear disulfide cystamine (CA) - sensitized by the excited triplet state of 3-carboxybenzophenone (3CB). Kinetic analysis reveals that the quenching rate constant for DHDT (k_q = 8.5×10^9 M^{-1}s^{-1}) is significantly higher than that for linear CA (k_q = 3.9×10^9 M^{-1}s^{-1}) mirroring structural reactivity trends previously observed with both $^1O_2$ and two-electron oxidants. In contrast to previous studies, direct spectroscopic identification of primary intermediates, including the disulfide radical-cation (– S$^{\bullet+}$–S–; identified as a transient absorption at ~ 380 nm) and the 3CB radical anion (broad absorption at ~ 600 nm) was achieved on a nanosecond timescale. Stable products arising from decay of the disulfide radical-cation were determined by LC-MS/MS, with three competing mechanistic pathways identified: (i) deprotonation yielding carbon-centred α-thioalkyl radicals and subsequent αS-αS dimers; (ii) disulfide (S-S) bond cleavage leading to products containing a single sulfur atom; and (iii) carbon-sulfur (C-S) bond cleavage which fragments the molecule whilst leaving the disulfide bridge intact. These findings provide a comprehensive map of the early events and subsequent free-radical cascades of disulfide oxidation, offering essential insights into the light-induced degradation of disulfide-containing proteins.

1. Introduction

The sulfur-containing amino acids methionine (Met), cysteine (Cys) and cystine (the disulfide formed from Cys) are fundamental components of the proteome and are uniquely susceptible to oxidative modification due to the high reactivity of their sulfur centers.[1, 2] Of these, oxidation of the thiol/thiolate group of Cys,[3, 4] and the thioether moiety of Met [5, 6] have been a primary focus of redox biology because their oxidation is a hallmark of an altered redox environment, aberrant cell signaling, biological aging and is a central factor in many pathologies associated with chronic or acute inflammation, including cardiovascular diseases and neurodegenerative conditions such as Parkinson's and Alzheimer's diseases.[2] With regard to the last of these, oxidation of Met35 in the C-terminal domain of β-amyloid (Aβ) within the brain is thought to trigger protein aggregation and the neurotoxicity associated with amyloid plaques.[7] As a consequence, the one-electron oxidation pathways of thioethers-including the formation of sulfur radical-cations, [8] their stabilization through three-electron bonds,[9] and their decay via deprotonation or decarboxylation [10] have been extensively explored. Similarly, a large volume of data is available on the oxidation of Cys by both radical and two-electron oxidants,[11] the large range of products generated by these reactions [12] (e.g. disulfides, oxy-acids, adduct species), and the consequences of such processes for normal cellular physiology and pathology.[13]

In contrast, the oxidation of disulfide bonds, which are formed from the oxidation of two Cys residues, is less well characterized despite the critical role of these species in maintaining biological structures (e.g. in extracellular matrix formation, receptors and structural proteins, plasma proteins), as allosteric regulators of protein activity,[14] and in the catalytic cycle of many enzymes (e.g. thioredoxins, peroxiredoxins, glutathione peroxidases).[15] Disulfides act as permanent "staples" that stabilize the three-dimensional folding of ~ 21% of all proteins. These linkages are particularly abundant in extracellular matrix proteins and receptors, where they maintain the distance and angle constraints required for biological activity.[16] Modification of disulfides is not only associated with a loss of protein function and biological activity but also poses major industrial challenges including the degradation of therapeutic antibodies and vaccines, and the spoilage of food and beverages.[17] Despite the importance of these species and the implications of their modification, the specific structural and mechanistic factors that control disulfide oxidation have not been studied to the same depth as their thiol and thioether counterparts.

A limited number of kinetic and product studies have been conducted of disulfide oxidation, though these have primarily been conducted with two-electron oxidants (e.g. H_2O_2, HOCl, HOBr, ONOOH) [18, 19] and singlet oxygen ($^1O_2$) [20] and not radical (one-electron) species.[21] These studies indicate that the rate constants for oxidation vary markedly with the disulfide structure (cyclic versus linear) and the presence of suitably positioned electron-donating groups that can stabilize the charged transient intermediates. Whether this is also true for triplet state and radical oxidation is unclear; though evidence is available for the formation of disulfide radical-cations.[8]

The chemistry of sulfur radical-cations is defined by their near-unique ability to form two-center three-electron (2c,3e) bonds with neighboring or remote electron-rich centers, such as sulfur, nitrogen, or oxygen atoms.[10] These transannular and intermolecular interactions provide a critical mechanism for the stabilization of the localized positive charge, significantly influencing the kinetic stability and subsequent reaction pathways. While such stabilization is well-documented for radical-cations from thioethers (e.g. dialkyl sulfides), which have been utilized as models for Met oxidation,[10] the behavior of disulfide radical-cations—specifically those involving a π-type radical system[8] - represents an under-researched and vital area of study within biological systems. The fate of these transients and whether they undergo α-deprotonation, C-S bond scission, or complex structural rearrangements (as seen with thioether radical-cations), is likely to be dictated by their molecular geometry and the degree of orbital overlap that can be achieved within hypervalent frameworks. Understanding these radical motifs is essential for deciphering the complex events that follow the initial oxidation of a disulfide in sulfur-rich biomolecular environments.

Light-induced oxidative damage, mediated by photosensitizers, represents a significant pathway for the degradation of disulfides. Benzophenone (BP) and its water-soluble derivatives, such as 3-carboxybenzophenone (3CB),[22, 23] are ideal tools for studying these processes. These sensitizers exhibit selective UVA activation (350–370 nm) and high intersystem crossing yields (ϕ_{isc} ~ 1), allowing for the targeted generation of reactive species without direct photo-oxidation of the protein backbone. In

these systems, the excited triplet sensitizer acts as a potent one-electron oxidant, accepting an electron from the sulfur moiety to form a charge-transfer complex. Previous studies using $^1O_2$,[20] a key intermediate in photooxidation, has revealed that the overall rate constants for $^1O_2$ quenching (total of physical and chemical processes) by disulfides vary by nearly three orders of magnitude, with cyclic structures showing higher quenching rate constants than linear chains.

This study aims to address this knowledge gap with regard to disulfide one-electron oxidation by providing a detailed mechanistic investigation of the one-electron oxidation of model disulfides. By utilizing laser flash photolysis (LFP) and high-resolution LC-MS/MS, the early events and stable products of 3CB-sensitized oxidation have been characterized for two model compounds: the cyclic disulfide trans-4,5-dihydroxy-1,2-dithiane (DHDT) and the linear species, cystamine (CA). The use of LFP has allowed real-time data to be obtained for the formation of disulfide radical-cations, allowing us to map the subsequent free-radical cascade and product formation. By comparing these kinetic data and product distributions, we elucidate how structural factors such as ring strain and orbital overlap influence the susceptibility of disulfide bridges to light-induced damage.

2. Experimental Section

2.1. Materials

3-Carboxybenzophenone (3CB) was obtained from Sigma-Aldrich at the highest available grade and used as received. *Trans*-4,5-Dihydroxy-1,2-dithiane (DHDT) and cystamine (CA) were utilized as model disulfides. All aqueous solutions were prepared using deionized water from a Millipore Simplicity system (Billerica, MA, USA). The pH of the solutions was adjusted to 9–10 with KOH solution to favor the formation of the 3CB radical anion.

2.2. Laser flash photolysis (LFP)

The nanosecond LFP setup has been described in detail previously[24]. Transient species were generated using 340 nm excitation. The light source was a primoScan OPO (GWU-Lasertechnik, Germany) pumped by the third harmonic of a Nd:YAG laser (Quantel, Q-smart 450) with a pulse duration of 8–10 ns and pulse energy maintained at approximately 2 mJ to minimize multi-photonic processes. The monitoring system comprised a 150 W pulsed Xe lamp (Hamamatsu, E7536) as the probe source, a monochromator (Princeton Instruments, Spectra Pro SP-2155), and an R955 photomultiplier (Hamamatsu). Data acquisition was performed using a 350 MHz digital oscilloscope (Tektronix, MDO 3024) triggered by a fast photodiode (Thorlabs, DET10M, ~ 1 ns rise time). The system was controlled via LabView 8.0 software. Transient absorption kinetic traces were recorded from 370 to 700 nm at 10 nm intervals for samples containing 4 mM 3CB and 10 mM quencher (DHDT or CA).

2.3. Steady-state photolysis and LC-MS analysis

Stationary irradiation was performed in 1 cm × 1 cm quartz cells using a Genesis CX355 STM OPSL laser (Coherent) emitting at 355 nm with an output power of 50 mW. To ensure oxygen-free conditions, all solutions were purged with high-purity argon for at least 30 minutes prior to and during irradiation. Post-irradiation samples were analyzed using an Ultimate 3000 UHPLC system (Thermo Scientific/Dionex). Separation was achieved on a C18 reversed-phase column (2.6 µm, 2.1 mm × 100 mm) maintained at 40°C. The mobile phase consisted of water (A) and acetonitrile (B), both containing 0.1% (v/v) formic acid. A linear gradient from 7% to 80% B was applied over 42 minutes at a flow rate of 0.3 mL/min. The UHPLC was coupled to a Bruker Impact HD QTOF mass spectrometer. Ions were generated via electrospray ionization (ESI) in positive mode. Structural characterization of photoproducts was performed using collision-induced dissociation (CID) with nitrogen gas in the Q2 section to obtain MS/MS fragmentation patterns.

3. Results and Discussion

3.1. Determination of quenching rate constants

The primary step in the sensitized photooxidation of disulfides involves the quenching of the excited triplet state of 3-carboxybenzophenone (^{3}3CB*) by the sulfur center. The quenching rate constants (k_q) were determined from Stern-Volmer plots using the 3CB triplet decay monitored at 520 nm. For the cyclic disulfide DHDT, k_q was calculated to be 8.5×10^9 $M^{-1}s^{-1}$, whereas for the linear species cystamine (CA), the value was significantly lower at 3.9×10^9 $M^{-1}s^{-1}$ (Fig. S1).

These data indicate that cyclic disulfides exhibit higher reactivity toward the 3CB triplet than linear ones, mirroring the trend reported previously for the quenching of $^1O_2$.[16, 18, 20] In that study, and also studies on other two-electron oxidants, the higher reactivity of 5- and 6-membered cyclic disulfides was attributed to better orbital overlap between the neighboring sulfur lone pair and the developing zwitterionic intermediate (hyperconjugation), a structural advantage less prevalent in linear chains, and more favorable for 5- than 6-membered rings due to better orbital overlap.

3.2. Early photochemical events and transient species identification

LFP experiments (using 340 nm excitation) were employed to characterize the transient intermediates formed immediately following the laser pulse and the results obtained are illustrated in Figs. 1 and 2. The initial spectrum (Fig. 1; 11–20 ns after the pulse) exhibits two distinct absorption bands: (i) at ~ 520 nm, assigned to the excited triplet state of the photosensitizer (^{3}3CB*); and (ii) at 380–390 nm, assigned to the primary sulfur radical-cation (DHDT$^{\bullet+}$), formed via one-electron transfer from the disulfide to ^{3}3CB* to give the corresponding 3CB radical-anion (3CB$^{\bullet-}$). The assignment of the transient absorption band near 380 nm to a disulfide-derived intermediate is consistent with the work of Elliot *et al.*,[25]who observed a nearly identical feature peaking at around 380–390 nm following the one-electron oxidation

of amino-containing disulfides including cystamine. In this previous study, this signal was attributed to oxidation intermediates - tentatively identified as perthiyl radicals or stabilized disulfide radical-cations. While sulfur-centered thioether radical-cations (e.g., from Met) and their stabilized three-electron bonded dimers $(S\therefore S)^+$ are well-documented, [8]the transient absorption signatures of the corresponding disulfide radical-cations ($DHDT^{\bullet+}$ and $CA^{\bullet+}$) have not been observed previously in photosensitized systems, to the best of our knowledge. The assignment of the 380 nm absorption to the radical-cation, is supported by the simultaneous decay of the photosensitizer triplet state (~ 520 nm) with matching kinetics. The high sensitivity of the LFP system allowed characterization of these species despite their rapid decay on a nanosecond timescale, a transient window that has previously been elusive for spectroscopic detection. These direct observations confirm that the initial oxidative event is a one-electron transfer, creating a highly reactive electron-deficient disulfide-derived center that subsequently triggers the bond cleavage and deprotonation pathways (see below).

The decay of the 520 nm triplet signal occurs simultaneously with the growth of the 380 nm band, with kinetics matching those calculated from the Stern-Volmer equation. Within tens of nanoseconds (Fig. 1c 19–75 ns), these primary signals decay rapidly, giving rise to a persistent broad absorption band peaking around 600 nm, assigned to $3CB^{\bullet-}$, confirming that the triplet quenching mechanism of DHDT proceeds via one-electron rather than hydrogen atom transfer.

In the case of the linear cystamine (CA) system, the transient spectroscopic behavior suggests a different quenching pathway. Following the triplet quenching of $3CB^*$ by CA (Fig. 2a,b), the transient absorption spectra at longer delay times reveal a broad band peaking around 530–550 nm. This feature is characteristic of the protonated 3CB ketyl radical ($3CBH^{\bullet}$), in contrast to the radical anion ($3CB^{\bullet-}$) peaking around 600 nm observed for DHDT. This indicates that the quenching of CA proceeds via a proton-coupled path - either stepwise electron transfer followed by rapid proton transfer within the solvent cage, or a simultaneous process. This variation in the quenching mechanism can be rationalized by the conformation of the respective encounter complexes $[3CB\cdots disulfide]^{\ddagger}$. For the flexible linear CA, the encounter complex can be stabilized by hydrogen-bonding interactions between the unprotonated amino groups of the quencher and the carbonyl or carboxylate oxygen of the sensitizer (see Fig S2 for a schematic drawing of the two complexes). This close proximity likely facilitates efficient, base-assisted proton transfer to the sensitizer within the solvent cage. Conversely, in the cyclic DHDT system, the rigid dithiocyclohexane ring and steric constraints restrict such stabilizing H-bonding and favorable spatial alignment. Consequently, proton transfer within the DHDT encounter complex is less favored, allowing purely one-electron transfer (charge separation) to dominate, as evidenced by the persistent signature of the free $3CB^{\bullet-}$ radical anion.

3.3. Mechanistic pathways and product identification by LC-MS

The rapid decay of the disulfide radical-cation suggests it undergoes fast chemical transformations. Analysis of the stable post-irradiation products by LC-MS has provided evidence for the occurrence of

three competing primary decay pathways (Scheme 1). Examples of the chromatograms and the corresponding MS/MS data supporting the identifications are provided in Figs. 3 (DHDT) and 4 (CA).

The first decay pathway is deprotonation in which $DHDT^{\bullet+}$ and $CA^{\bullet+}$ undergo proton transfer to $3CB^{\bullet-}$ or the bulk medium, yielding a carbon-centered α-thioalkyl radical ($\alpha S^{\bullet}$). These αS radicals dimerize to form stable products which were detected by LC-MS. For $DHDT^{\bullet+}$, this is evidenced by a dimeric product P1 (with *m/z* 302.9857), identified by its exact mass and an isotopic profile confirming the presence of four sulfur atoms (18.87%). Similarly, for $CA^{\bullet+}$, this path leads to the radical coupling product P5 (*m/z* 379.1145).

The second identified decay process involves disulfide (S-S) bond cleavage. This reaction path leads to products containing only a single sulfur atom. For $DHDT^{\bullet+}$, S-S cleavage yields ring-opened intermediates that ultimately form product P2 (*m/z* 334.9579) and its dehydrated form P3 (*m/z* 316.9476). For $CA^{\bullet+}$, this pathway results in product P6 (*m/z* 330.1170).

The third pathway involves carbon-sulfur (C-S) bond cleavage. A particularly notable feature is that some of the detected products retained an unbroken disulfide moiety, with photoproduct P4 (*m/z* 215.9326) detected from $DHDT^{\bullet+}$, while the product P7 (*m/z* 270.1123) from $CA^{\bullet+}$ does not contain disulfide bond at all (see Tables S3 in SI section). Use of high-resolution MS was critical to these analyses, as it allowed precise determination of the number of sulfur atoms via isotopic profiles, and therefore allowed unambiguous assignment of the product species. Together these data demonstrate that the one-electron oxidation of disulfides leads to a complex cascade of reactions (see Schemes 2 and 3) that result in significant structural modification and bonds cleavage.

The differences in the chromatograms and the relative yields (see Table S1 and S2 in SI section) of the stable photoproducts - specifically, the fact that the yield of the deprotonation dimer (P1 for DHDT) is approximately one order of magnitude higher than the corresponding deprotonation product (P5 for CA) - can be intuitively rationalized by the structural stability, steric effects, and conformational dynamics of their respective radical cations.[26] In the cyclic DHDT system, the rigid ring framework imposes severe conformational constraints that restrict the outward movement of the sulfur atoms. This ring-confinement effect acts as an internal "restoring force" that holds the sulfur atoms in close proximity, making S–S bond cleavage in the DHDT radical cation relatively slow or highly reversible. Consequently, the cyclic radical cation is structurally stabilized, which prolongs its effective lifetime and allows the competitive deprotonation pathway to occur much more efficiently, leading to the prominent yield of the dimeric product P1.

In contrast, the linear CA radical cation lacks any cyclic framework or restoring forces to hold the sulfur atoms together. Upon oxidation, the straight-chain system allows the sulfur atoms to separate rapidly and irreversibly. This fast bond scission heavily outcompetes deprotonation, thereby suppressing the formation of the P5 deprotonation product by an order of magnitude (compared to the respective P1). Furthermore, steric and geometric factors in the rigid, cyclic DHDT may keep the relevant α-protons in a

highly favorable orientation for transfer, whereas the high flexibility of the linear CA chain provides no such steric disadvantage to counteract the dominant, rapid bond-rupture pathways.

4. Conclusions

The present study provides a detailed, time-resolved and steady-state mechanistic investigation into the photosensitized one-electron oxidation of model disulfides, demonstrating how structural and conformational factors dictate both the early photophysical events and the subsequent free-radical reaction cascades. The findings of this work lead to the following primary conclusions:

Spectroscopic Identification of Primary Disulfide Transients

This study achieves the first direct spectroscopic identification of the primary disulfide radical cation (–$S^{\bullet+}$–S–) in a photosensitized system on a nanosecond timescale. Laser flash photolysis (LFP) experiments successfully captured a characteristic transient absorption band peaking at ~380 nm, which decays rapidly within tens of nanoseconds with kinetics that match the photosensitizer triplet state (^{3}3CB*) decay. This observation provides real-time, definitive proof of the initial one-electron transfer event and aligns with pulse radiolysis literature of related amino-containing disulfides.

Kinetics of Triplet Quenching and Geometry-Dependent Reactivity

The kinetics of triplet state quenching are heavily influenced by the molecular geometry of the disulfide quencher. The quenching rate constant (k_q) for the cyclic disulfide DHDT (8.5×10^9 $M^{-1}s^{-1}$) is significantly higher than that for the linear Cystamine ($k_q = 3.9\times10^9$ $M^{-1}s^{-1}$). This trend closely mirrors structural reactivity patterns observed previously with singlet oxygen ($^1O_2$) [20] and two-electron oxidants,[16, 18, 20] where cyclic 5- and 6-membered systems benefit from enhanced orbital overlap between the neighboring sulfur lone pair and the developing charge-transfer transition state.

Mechanistic Divergence in the Excited State Encounter Complex

Divergence in the reduction products of the photosensitizer at longer times - yielding the free radical anion $3CB^{\bullet-}$ at ~600 nm for DHDT compared to the protonated ketyl radical $3CBH^{\bullet}$ at ~530–550 nm for CA - is successfully rationalized by the geometry and stabilization of their respective excited-state encounter complexes [3CB···disulfide]‡. For flexible linear CA, the encounter complex is stabilized by hydrogen-bonding interactions between the unprotonated amino groups of the quencher and the carbonyl/carboxylate oxygen of the sensitizer, facilitating efficient, base-assisted proton transfer in the solvent cage. Conversely, the rigid dithiacyclohexane ring of DHDT imposes steric constraints that restrict such stabilizing H-bonding, thereby suppressing proton transfer and allowing pure one-electron transfer (charge separation) to dominate.

Structural Control of Intermediate Partitioning (Conformational Dynamics vs. Fast Dissociation): The subsequent thermal cascade of the disulfide radical cation undergoes competitive partitioning among

three distinct pathways: deprotonation, disulfide (S–S) bond cleavage, and carbon–sulfur (C–S) bond cleavage. The relative yields of these pathways are profoundly controlled by the conformational dynamics of the intermediate radical cations:

1. In cyclic DHDT, the rigid framework imposes a ring-confinement effect, which acts as an internal "restoring force" that holds the sulfur atoms in close proximity, making S–S cleavage slow or highly reversible. This structurally stabilizes the radical cation, prolonging its lifetime and allowing the competitive deprotonation pathway to proceed with high efficiency, dominating the product yield as the αS − αS dimeric product P1 (yield contribution ∼62.4%).
2. In linear CA, the lack of a cyclic framework or restoring forces allows the sulfur atoms to separate rapidly and irreversibly. This fast bond scission heavily outcompetes deprotonation, thereby suppressing the deprotonation dimer P5 to a minor fraction (yield contribution ∼7.3%).

Precision Mass Spectrometry for Product Elucidation

High-resolution mass spectrometry (LC-MS/MS) and exact mass measurements were critical in distinguishing the stable markers of these competitive pathways. By determining the exact molecular composition and isotopic profiles (such as confirming the presence of four sulfur atoms in P1 photoproduct), this work successfully maps the complete cascade of free-radical reactions following disulfide oxidation. This provides essential insights into the structural factors that govern light-induced protein degradation and biological stability.

Declarations

Author Contribution

T.P. and M.B. wrote the main manuscript text, M.I-K and P.F. prepared figures and schemes, M.B. did the MS experiments, P.F. and T.P. did the LFP experiments, M.J.D. and T.P. - conceptualization and design of work, T.P. and M.J.D. - supervision. All authors reviewed the manuscript.

Acknowledgement

The authors are grateful the project: “Excellence Initiative – Research University” support for the internationalization of scientific research (ID-UB, grant no. 158/13/UAM/0043), the Novo Nordisk Foundation (NNF grant: NNF20SA0064214) and the Independent Research Fund Denmark - Technology and Production (DFF, grant: 4286-00216B) for financial support.

Data Availability

The authors declare that the data supporting the findings of this study are available within the paper and its Supplementary Information files. Should any raw data files be needed in another format they are available from the corresponding author upon reasonable request.

References

1. Thornton, J. M. (1981). Disulphide Bridges in Globular Proteins. *Journal Of Molecular Biology*, *151*, 261–287. 10.1016/0022-2836(81)90515-5
2. Davies, M. J. Protein oxidation and peroxidation. *Apr 01 2016 Portland Press Ltd*. 10.1042/BJ20151227
3. Yang, J., Carroll, K. S., & Liebler, D. C. (2016). The expanding landscape of the thiol redox proteome. *Jan 01*. 10.1074/mcp.O115.056051. American Society for Biochemistry and Molecular Biology Inc.
4. Poole, L. B. (2015). The basics of thiols and cysteines in redox biology and chemistry. *Elsevier Inc*. 10.1016/j.freeradbiomed.2014.11.013
5. Pedzinski, T., Grzyb, K., Kaźmierczak, F., Frański, R., Filipiak, P., & Marciniak, B. (2020). Early Events of Photosensitized Oxidation of Sulfur-Containing Amino Acids Studied by Laser Flash Photolysis and Mass Spectrometry, *Journal of Physical Chemistry B*, vol. 124, no. 35, pp. 7564–7573, Sep. 10.1021/acs.jpcb.0c06008
6. Pedzinski, T., Markiewicz, A., & Marciniak, B. (Apr. 2009). Photosensitized oxidation of methionine derivatives. Laser flash photolysis studies. *Research on Chemical Intermediates*, *35*(4), 497–506. 10.1007/s11164-009-0046-4
7. Schöneich, C. (Jan. 2002). Redox processes of methionine relevant to β-amyloid oxidation and Alzheimer's disease. *Archives Of Biochemistry And Biophysics*, *397*(2), 370–376. 10.1006/abbi.2001.2621
8. Glass, R. S. (1999). Sulfur Radical Cations, *Topics in Current Chemistry*, vol. 205, pp. 1–87. 10.1007/3-540-48986-X
9. Asmus, K. D. (1990). *Sulfur-Centered Three Electron Bonded Radical Species in Chemistry and Biology*. Plenum. 10.1007/978-1-4684-5874-9_14
10. Grzyb, K., Sehrawat, V., & Pedzinski, T. (2023). The Fate of Sulfur Radical Cation of N-Acetyl-Methionine: Deprotonation vs. Decarboxylation, *Photochem*, vol. 3, no. 1, pp. 98–108, Mar. 10.3390/photochem3010007
11. Reddie, K. G., & Carroll, K. S. (Dec. 2008). Expanding the functional diversity of proteins through cysteine oxidation. *Current Opinion In Chemical Biology*, *12*, 611–618. 10.1016/j.cbpa.2008.07.028
12. Sies, H., et al. (Jul. 2022). Defining roles of specific reactive oxygen species (ROS) in cell biology and physiology. *Nature Reviews Molecular Cell Biology*, *23*(7), 499–515. 10.1038/s41580-022-00456-z
13. Fra, A., Yoboue, E. D., & Sitia, R. (2017). Cysteines as redox molecular switches and targets of disease. *Frontiers In Molecular Neuroscience*, *10*(06), 167. 10.3389/fnmol.2017.00167

14. Carroll, L., et al. (Nov. 2020). Oxidant-induced glutathionylation at protein disulfide bonds. *Free Radical Biology And Medicine*, *160*, 513–525. 10.1016/j.freeradbiomed.2020.08.018
15. Klomsiri, C., Karplus, P. A., & Poole, L. B. (2011). Cysteine-Based Redox Switches in Enzymes. *Antioxidants & Redox Signaling*, *14*, 1065–1081. 10.1089/ars.2010.3379
16. Karimi, M. (2016). Dec., Reactivity of disulfide bonds is markedly affected by structure and environment: Implications for protein modification and stability, *Sci. Rep.*, vol. 6. 10.1038/srep38572
17. Krämer, A. C., Torreggiani, A., & Davies, M. J. (Nov. 2017). Effect of Oxidation and Protein Unfolding on Cross-Linking of β-Lactoglobulin and α-Lactalbumin. *Journal Of Agriculture And Food Chemistry*, *65*(47), 10258–10269. 10.1021/acs.jafc.7b03839
18. Karimi, M., Crossett, B., Cordwell, S. J., Pattison, D. I., & Davies, M. J. (2020). Characterization of disulfide (cystine) oxidation by HOCl in a model peptide: Evidence for oxygen addition, disulfide bond cleavage and adduct formation with thiols, *Free Radic. Biol. Med.*, vol. 154, pp. 62–74, Jul. 10.1016/j.freeradbiomed.2020.04.023
19. Jiang, S., Carroll, L., Rasmussen, L. M., & Davies, M. J. (Jan. 2021). Oxidation of protein disulfide bonds by singlet oxygen gives rise to glutathionylated proteins. *Redox Biology*, *38*. 10.1016/j.redox.2020.101822
20. Gao, Q., Grzyb, K., Gamon, L. F., Ogilby, P. R., Pędziński, T., & Davies, M. J. (2023). The structure of model and peptide disulfides markedly affects their reactivity and products formed with singlet oxygen, *Free Radic. Biol. Med.*, vol. 207, pp. 320–329, Oct. 10.1016/j.freeradbiomed.2023.08.024
21. Trujillo, M., Alvarez, B., & Radi, R. (Feb. 2016). One- and two-electron oxidation of thiols: mechanisms, kinetics and biological fates. *Free Radical Research*, *50*(2), 150–171. 10.3109/10715762.2015.1089988
22. Pedzinski, T., et al. (Aug. 2014). 3-Carboxybenzophenone (3-CB) as an efficient sensitizer in the photooxidation of methionyl-leucine in aqueous solutions: Spectral, kinetic and acid-base properties of 3-CB derived transients. *Journal Of Photochemistry And Photobiology. A, Chemistry*, *287*, 1–7. 10.1016/j.jphotochem.2014.04.004
23. Bobrowski, K., Marciniak, B., & Hug, G. L. (1992). 4-Carboxybenzophenone-Sensitized Photooxidation of Sulfur-Containing Amino Acids. Nanosecond Laser Flash Photolysis and Pulse Radiolysis Studies. *Journal Of The American Chemical Society*, *114*, 10279–10288. 10.1021/ja00052a024
24. Pedzinski, T., Markiewicz, A., & Marciniak, B. (Apr. 2009). Photosensitized oxidation of methionine derivatives. Laser flash photolysis studies. *Research on Chemical Intermediates*, *35*(4), 497–506. 10.1007/s11164-009-0046-4
25. Elliot, A. J., Mceachern, R. J., & Armstrong, D. A. (1981). Oxidation of Amino-Containing Disulfides by Br2 and OH. A Pulse-Radiolysis Study. *Journal Of Physical Chemistry*, *85*, 68–75. 10.1021/j150601a015
26. Stephansen, A. B., Larsen, M. A. B., Klein, L. B., & Sølling, T. I. (Oct. 2014). On the photostability of the disulfide bond: An electronic or a structural property? *Chemical Physics*, *442*, 77–80. 10.1016/j.chemphys.2014.02.005

Scheme

Scheme 1, 2 & 3 are available in the Supplementary Files section.

Figures

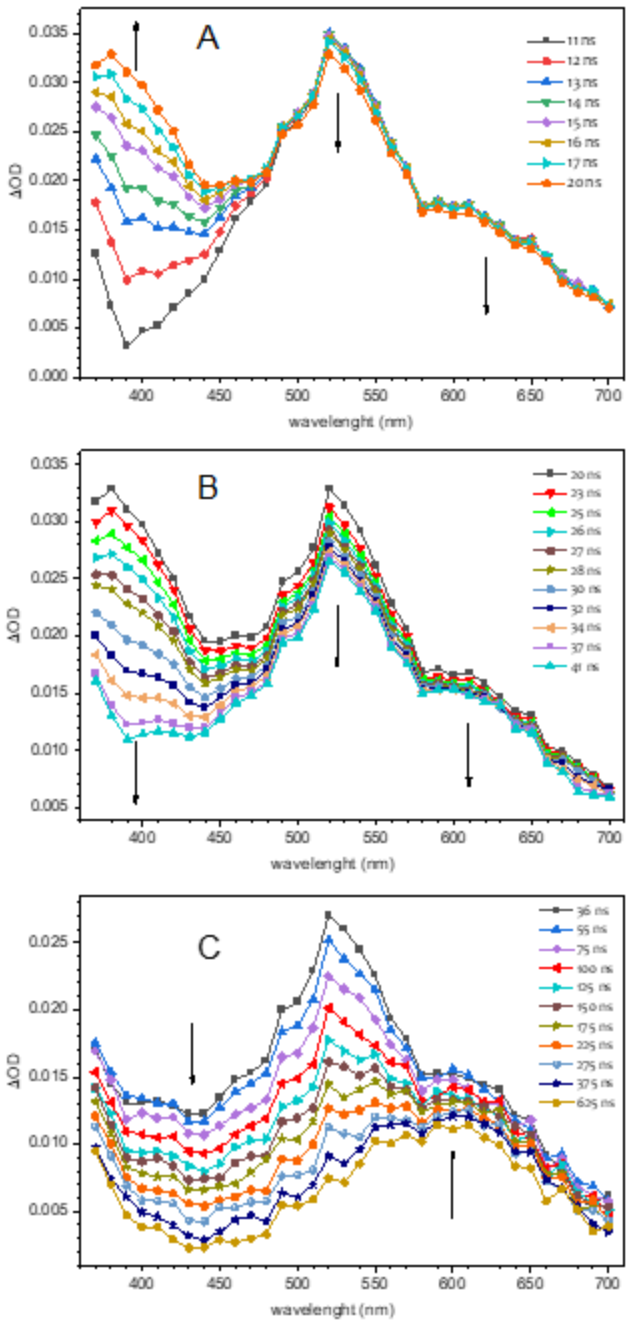


Figure 1

Time-evolution of transient absorption spectra detected on laser flash photolysis (at 340 nm) of DHDT (10 mM) in aqueous solution at pH 9-10. Panel A): After excitation using a laser pulse duration of ~10 ns a build-up of 2 absorption bands at ~380 nm and ~520 nm is detected. The signal at 520 nm is assigned

to the excited triplet state of the photosensitizer ($^{3}3CB^{*}$) while the signal around 380 nm is assigned to the disulfide radical-cation of DHDT ($DHDT^{\bullet+}$). Panels B, C: The signals detected immediately after the pulse (Panel a) decay rapidly within tens of nanoseconds and the only remaining signal is a broad absorption peaking around 600 nm assigned to the sensitizer radical-anion ($3CB^{\bullet-}$).

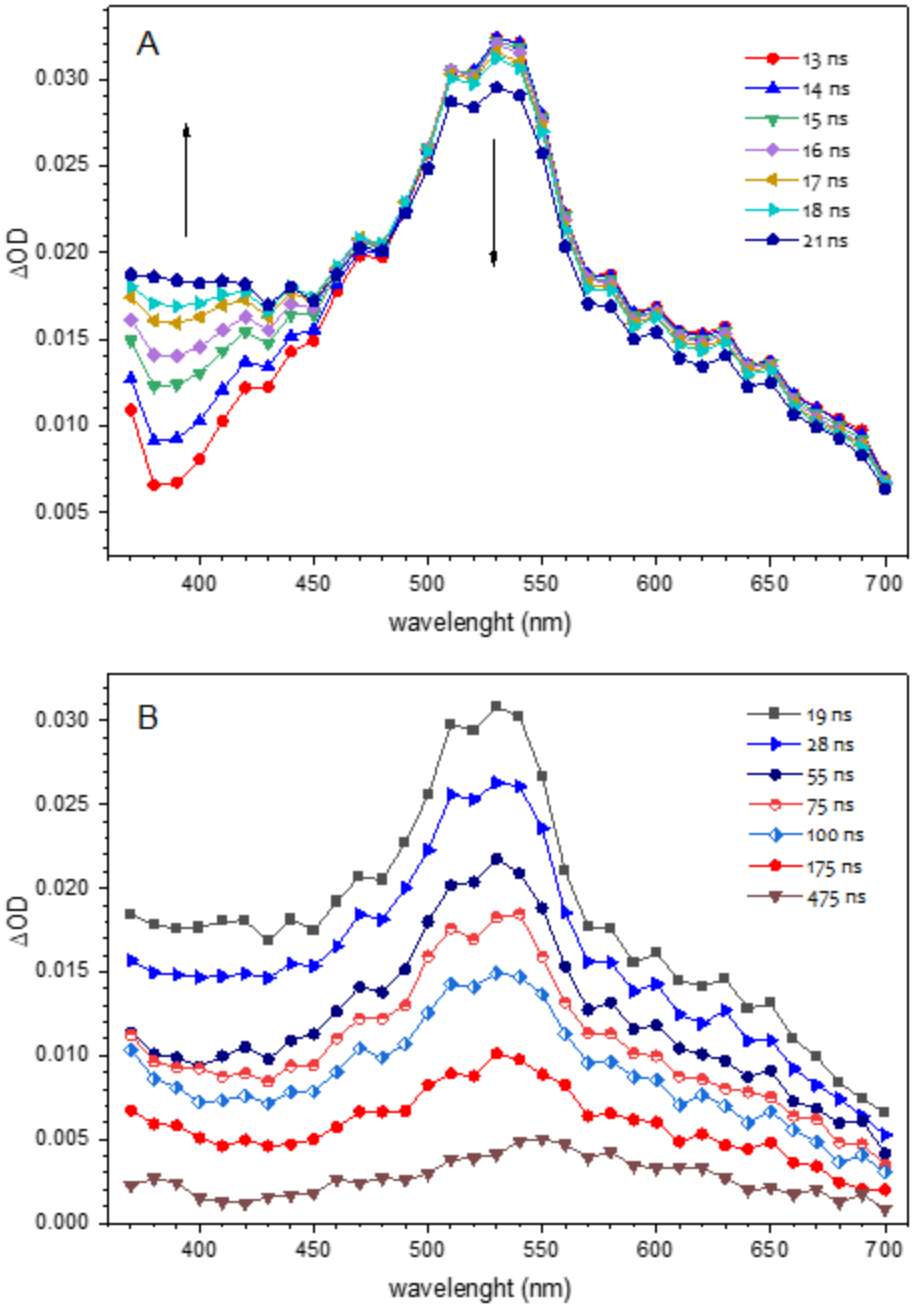


Figure 2

Time-evolution of transient absorption spectra detected on laser flash photolysis (at 340 nm) of CA (10 mM) in aqueous solution at pH 9-10. Panel A): After excitation using a laser pulse duration of ~10 ns a build-up of 2 absorption bands at ~400 nm and ~520 nm is detected. The signal at 520 nm is assigned to the excited triplet state of the photosensitizer ($^{3}3CB^{*}$) while the signal around 400 nm is assigned to

the disulfide-derived radical of CA ($CA^{\bullet+}$or its neutral alpha-thioalkyl radical). Panel B: The signals detected immediately after the pulse decay rapidly within tens of nanoseconds and the remaining signal is an absorption peaking around 530-540 nm assigned to the sensitizer's ketyl radical ($3CBH^{\bullet}$).

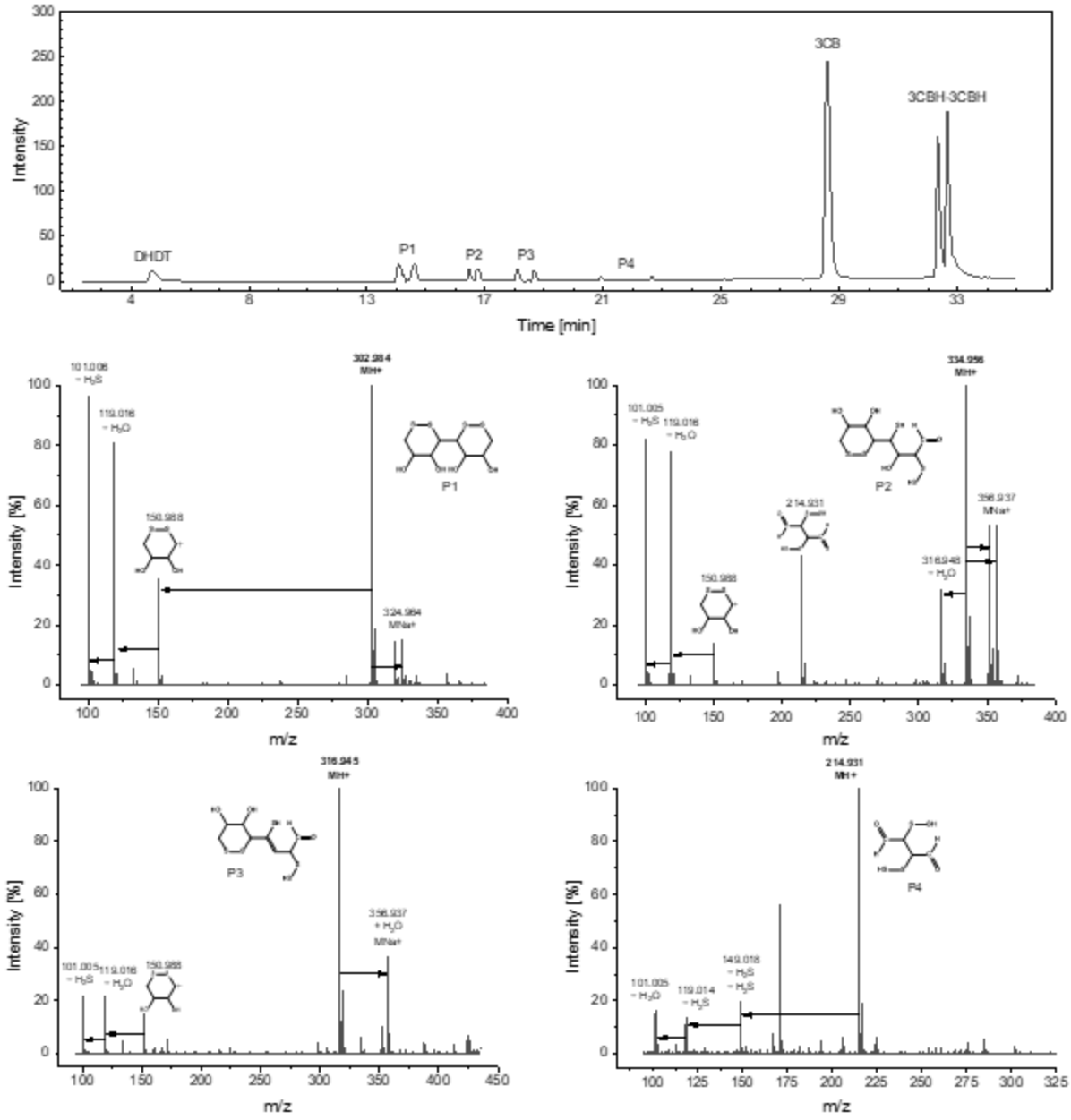


Figure 3

Chromatograms and MS spectra of detected photoproducts P1-P4 (DHDT)

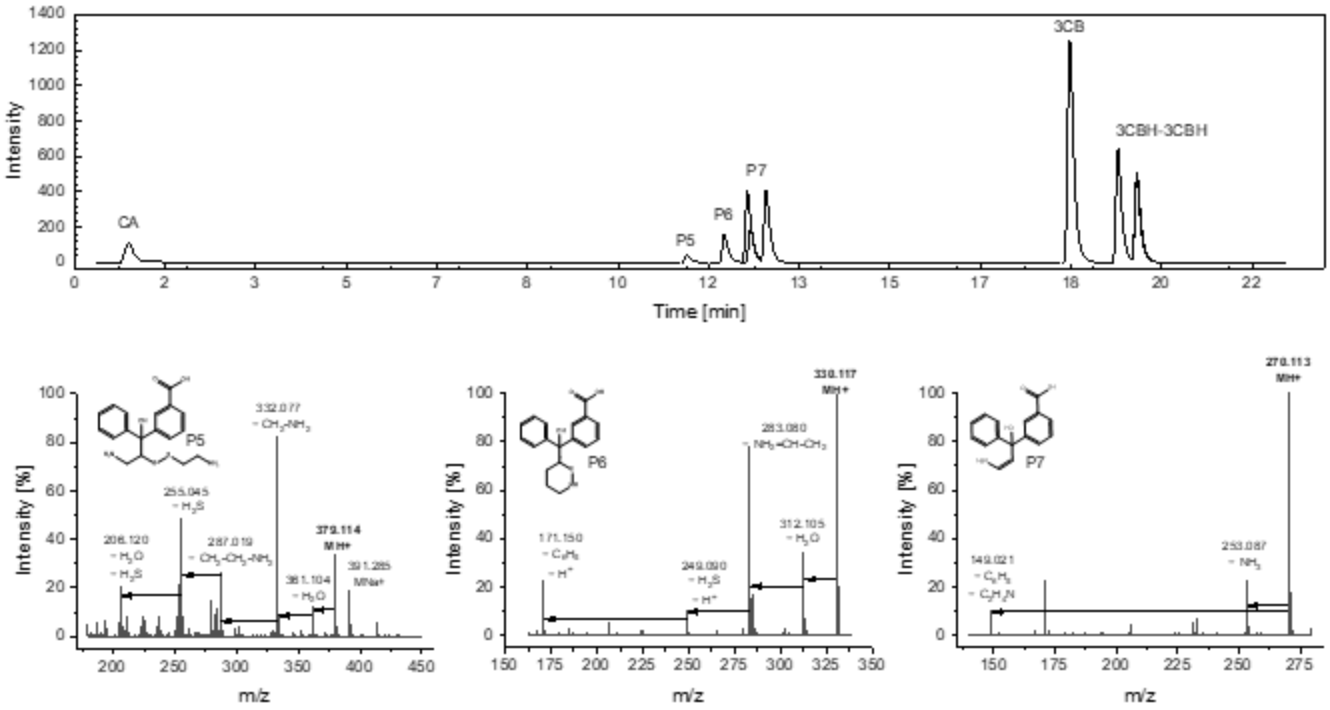


Figure 4

Chromatograms and MS spectra of detected photoproducts P5-P7 (CA)

Supplementary Files

This is a list of supplementary files associated with this preprint. Click to download.

- SupplementaryInformationJPPS.docx
- Scheme.docx